Photonic True-Time Delay Beamforming Using a Switch-Controlled Wavelength-Dependent Recirculating Loop

Jiejun Zhang, *Student Member, IEEE*, and Jianping Yao, *Fellow, IEEE, Fellow, OSA*

***Abstract*—A photonic true-time delay beamforming network to provide tunable progressive time delays for phased array beamforming is proposed and demonstrated. In the proposed system, a microwave signal is modulated on multiwavelength optical carriers and sent to an optical dispersive recirculating loop that contains a linearly chirped fiber Bragg grating (LCFBG) to provide a wavelength-dependent round trip time. As the microwave-modulated optical signals recirculate in the loop, the microwave signals carried by different wavelengths will experience different time delays at the output of the loop. By controlling the number of round trips, tunable progressive true-time delays are achieved, which are required for true-time delay phased array beamforming. The proposed true time delay beamforming network is experimentally evaluated. Two dispersive loops that can introduce a single-round-trip true-time delay difference of 2.5 ns and 160 ps are designed, which are implemented by using two LCFBGs with two different dispersion coefficients of 2500 and 200 ps/nm. The progressive time delays for beam steering achieved by the two dispersive loops can cover a beam scanning range from –60° to 60°.**

***Index Terms*—Dispersion, microwave photonics, phased array antenna, radar, true-time delay.**

I. Introduction

PHASED array antenna (PAA) plays a key role in modern radar systems as it can provide beam steering at a high speed without mechanical movement and with ultra-high directivity [1]. A beamforming network is required to produce progressive phase or time delays to the microwave signals to feed the array elements in a PAA, which can be implemented using phase shifters or true-time delay lines. The advantage of using true-time delay lines is that the beam is squint free, which is essential for broadband applications. The time delays can be realized using electronic delay lines but with a smaller bandwidth, a larger size and a higher loss [2]. For example, an electrical delay line having an electromagnetic bandgap structure was recently demonstrated on a 6.8-cm long chip, which has a bandwidth of 5 GHz, a maximum time delay of 750 ps and an insertion loss of over 5 dB [3]. The bandwidth cannot be further increased as strong ripples have already been seen in the bandwidth of the delay line. Photonics is considered a potential solution to implement true-time delays with greater bandwidth, smaller size and lower loss [4].

In the past few years, numerous photonic true-time delay beamforming networks have been demonstrated. In [5], a photonic true-time delay network based on free space optics was demonstrated. The time delay of a microwave signal modulated on an optical carrier is tuned by changing the polarization state of the optical carrier to make it travel along different optical paths with different time delays. As a free-space optical system generally requires a large number of mirrors and lenses, it is usually very heavy and bulky. Fiber optics and photonic integrated circuits can be used to mitigate these limitations thanks to the much smaller size and lower loss. In [6], a fiber Bragg grating (FBG) array was used to realize true-time delays. The tunability of the time delays was achieved by tuning the optical carrier wavelengths. A maximum true time delay of 233 ps was experimentally demonstrated. Since an FBG array contains a large number of discrete FBGs, to reduce the complexity, in [7] a true-time delay network using a single linearly chirped fiber Bragg grating (LCFBG) was proposed. Multiple optical carriers at different wavelengths with a uniform wavelength spacing are used, which, after modulation, are reflected by the LCFBG at different locations. Different time delays can be achieved for a microwave signal modulated on the optical carriers. Tunable time delay difference was achieved by tuning the wavelength spacing. The time delays can also be tuned by changing the chirp rate of the LCFBG. A time delay tuning range of 100 ps, with a tuning step of 1 ps was demonstrated. In [8], a dispersion compensating fiber was used instead of an LCFBG. Tunable true-time delays were achieved by changing again the wavelength spacing. Similarly, in [9] a single-mode fiber was used as a dispersive element to realize tunable time delays by changing the wavelength spacing of an optical frequency comb, which is used as the optical carriers. A fiber-optics-based beamforming network features a smaller size, but a tunable laser source (TLS) or tunable laser array (TLA) is usually required [6], [8], [9] to achieve tunable time delays, making the system costly, and beam scanning speed is limited by the wavelength tuning speed of the TLS or TLA. In addition, the wavelength stability due to wavelength tuning may be deteriorated, which will affect the time delay accuracy. In [10], instead of using a TLS or a TLA, a tunable dispersive medium based on the similar effect in [7] was used to implement tunable true-time delays. A true-time delay with a tuning range of 200 ps was demonstrated, which is still very limited. In [11], a multicore fiber was employed

Manuscript received February 08, 2016; revised May 26, 2016 and June 19, 2016; accepted June 21, 2016. Date of publication June 21, 2016; date of current version July 22, 2016. This work was supported by the Natural Sciences and Engineering Research Council of Canada. The work of J. Zhang was supported in part by a scholarship from the China Scholarship Council.

The authors are with the Microwave Photonics Research Laboratory, School of Electrical Engineering and Computer Science, University of Ottawa, Ottawa, ON K1N 6N5, Canada (e-mail: jpyao@eecs.uottawa.ca).

Color versions of one or more of the figures in this paper are available online at http://ieeexplore.ieee.org.

Digital Object Identifier 10.1109/JLT.2016.2583918

to achieve tunable true-time delays. By designing the refractive index profile of the multicore fiber, optical signals travelling in different cores will experience different time delays. Since the optical path lengths of the cores are fixed, the time delays cannot be conveniently tuned. Photonic true-time delays can also be realized based on the stimulated Brillouin scattering (SBS) effect in a fiber [12]. In the SBS gain spectrum, the time delay is wavelength dependent. By changing the optical wavelengths which are located within the SBS spectrum profile, the time delays are tuned. However, the spectral width of an SBS gain profile is very small, which would limit the bandwidth of the microwave signal to be time delayed. Other techniques to achieve true-time delays include the use of stack integrated micro-optical components [13]. Since movable prism groups are used, the reliability is poor. Recently, an on-chip microwave photonic beamformer based on Si_3N_4/SiO_2 waveguide technology was demonstrated [14], [15]. The stability is better than using fiber delay lines. Due to the small size of the chip, the achievable time delay is small, limited to a few hundreds of ps. In [16], a photonic microwave filter was designed to have a frequency response that is similar to a microwave delay line with a linear group delay response. However, the tunable range of the time-delay is only 31.9 ps. It was also demonstrated that a silicon chip with a low-loss spiral waveguide can achieve a time delay of 130 ns [17]. However, the time delay is fixed with no tunability, which is not applicable for true-time delay beamforming. For phased array beamforming, large tunable time delays are required to provide beam steering with a large scanning range.

In this paper, a simple fiber-optic true-time delay beamforming network is proposed and demonstrated to provide very large tunable progressive time delays at a high tuning speed. The large time delays are generated using a switch-controlled recirculating wavelength-dependent dispersive loop incorporating an LCFBG. Due to the multiple use of the LCFBG, the time delays can be large. Since only a single LCFBG and a laser array with fixed wavelengths are needed, the system is simpler and less costly. The tuning of the time delays can be performed by controlling the optical switch to allow the microwave-modulated optical signals to travel in the dispersive loop for a given number of round trips.

In the proposed system, a microwave signal, which should be pulsed with a pulse duration less than the round trip time of the recirculating dispersive loop, to be radiated is modulated on the multi-wavelength carriers from an array of laser diodes (LDs). The microwave-modulated optical signals are sent to a switch-controlled wavelength-dependent recirculating dispersive loop [18]. Since the optical signals modulated on different wavelengths are reflected at different locations of the LCFBG, different time delays are achieved. The tuning of the time delays are realized by controlling the number of round trips that the optical signals recirculate in the dispersive loop, which is done by using a 2×2 optical switch to direct the optical signals back to the loop for additional time delays or to the output of the loop. The proposed true-time delay beamforming network is experimentally demonstrated. A four-channel true-time delay beamforming network using two different recirculating dispersive loops with a single-round-trip true-time delay difference of 2.5 ns and 160 ps per round trip incorporating two LCFBGs with different dispersion coefficients of 2500 ps/nm and 200 ps/nm are demonstrated. The use of the beamforming network to generate tunable progressive true-time delays for phased arrayed beamforming that can cover a scanning range from –60° to 60° is demonstrated.

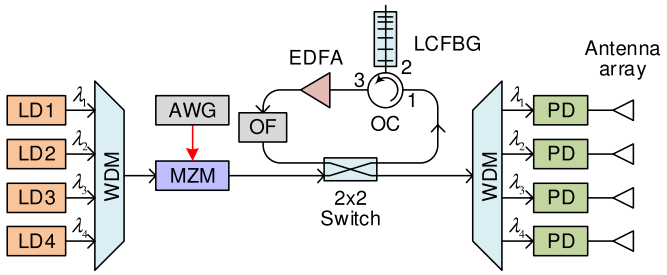

Fig. 1. Schematic diagram of the true-time delay beamforming network using a recirculating wavelength-dependent dispersive loop. LD: laser diode; WDM: wavelength-division multiplexer; AWG: arbitrary waveform generator; MZM: Mach-Zehnder modulator; OF: optical filter; EDFA: erbium-doped fiber amplifier; OC: optical circulator; LCFBG: linearly chirped fiber Bragg grating; PD: photodetector.

II. Principle

The schematic diagram of the proposed true-time delay beamforming network is shown in Fig. 1. The light waves from a laser array consisting of four LDs with four different wavelengths of λ_1 to λ_4 are combined at a wavelength-division multiplexer (WDM1) and sent to a Mach-Zehnder modulator (MZM), where a microwave feed signal, generated by an electrical arbitrary waveform generator (AWG), is modulated on the four wavelengths. The microwave-modulated optical signals at the output of the MZM are then launched into a switch-controlled wavelength-dependent optical dispersive recirculating loop through a 2×2 optical switch. An LCFBG is incorporated in the loop via an optical circulator (OC) to provide a wavelength-dependent time delay. An erbium-doped fiber amplifier (EDFA1) is also incorporated in the loop to compensate for the loss in the loop so that an optical signal can recirculate in the loop for multiple round trips. A programmable optical filter (OF) with four passbands centered at λ_1 to λ_4 is also employed to suppress the amplified spontaneous emission (ASE) noise from EDFA1. The number of round trips is controlled by the 2×2 optical switch. It is required that the optical switch can change its state within a time window with no signal travelling through it. This can be realized by a high-speed optical switch such as an electro-optic switch reported by us which has a sub-nanosecond switching time [19]. At the output of the loop, a second EDFA (EDFA2) is used to further amplify the optical signal and a second WDM (WDM2) is used to demultiplex the time-delayed optical signals, which are converted to four time-delayed microwave signals at the photodetectors (PDs), which are radiated to free space via the array elements in a PAA.

The microwave feed signal $x(t)$ from the AWG is modulated on the multi-wavelength optical carriers. The optical switch is first configured at the cross state, so that the

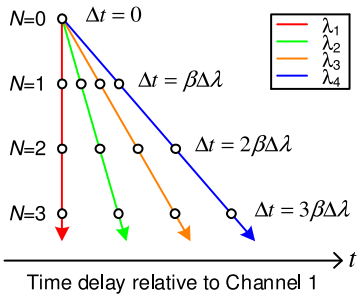

Fig. 2. The time delay of the signal in each channel relative to channel 1 as the number of round trips *N* increases.

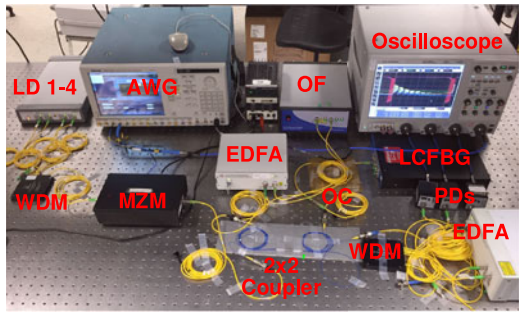

Fig. 3. The photograph of the experimental setup.

microwave-modulated optical signals at different wavelengths can be directed into the recirculating dispersive loop. After the signals enter the loop, the switch is changed to the bar state. Thus, the optical signals will be recirculating in the loop until the state of the switch is changed from the bar to the cross state. Depending on the number of round trips in the loop, the optical signals will experience different time delays.

Due to a wavelength-dependent time delay resulted from the LCFBG in the loop, the time delay for a wavelength $\lambda_i (i = 1, 2, 3, 4)$ is given by

$$T_i = t_0 + \beta\left(\lambda_i - \lambda_r\right) \tag{1}$$

where t_0 is the fixed time delay of the loop excluding the LCFBG; β is the dispersion coefficient of the LCFBG and λ_r is a reference wavelength which is equal to the wavelength of the lower end of the LCFBG connected to the optical circulator. Assuming that the microwave feed signal $x(t)$ recirculates in the dispersive loop for *N* round trips, a time delay signal given by $x_i(t - NT_i)$ can be achieved at the output of the loop. The time delay difference between the signals carried by two adjacent wavelengths, $x_i(t - NT_i)$ and $x_{i+1}(t - NT_{i+1})$, is given by

$$\Delta t = NT_{i+1} - NT_i = N\beta\Delta\lambda \tag{2}$$

where $\Delta\lambda$ is the wavelength spacing between two adjacent optical carriers. Note that the wavelengths are uniformly spaced in our system. It can be seen that progressive true-time delays can be obtain for the optical signals as the number of round trips *N* increases. The relationship between the time delays, the number of round trips and the carrier wavelengths are shown in Fig. 2. By increasing the number of round trips, a time-delay increment of $\beta\Delta\lambda$ can be achieved. A relationship between the beam steering angle and the number of round trips that the signals recirculates in the loop can then be written as [4]

$$\theta = \sin^{-1}\left(\frac{cN\beta\Delta\lambda}{d}\right) \tag{3}$$

where *d* is the spacing between two adjacent antenna elements in a PAA; *c* is the light velocity in vacuum. It can be seen that, as *N* increases, the beam pointing direction will be changed with a step determined by $\beta\Delta\lambda$ and a scanning range determined by the maximum value of *N*. In our system, *N* can be controlled to be a large finite number if the round trip loss in the loop can be fully compensated by EDFA1.

For radar applications, the radial resolution is determined by the time-bandwidth product of the radiated radar signal. It is required that a true-time delay system is capable of providing tunable time delays to a signal with not only a large bandwidth but also a long temporal duration [1]. In our system, it is required that the temporal duration of a microwave feed pulse should be smaller than the round trip time of the loop, so that two adjacent time-delayed pulses will not overlap when recirculate in the loop, i.e., the duration of the microwave feed signal should satisfy $\tau < t_0$. Thanks to the very low loss of an optical fiber, t_0 can be controlled large by using a long optical fiber in the loop. Note that the loop length cannot be chosen arbitrarily long, since a longer dispersive loop will slow down the beam steering speed. In addition to radial resolution, the angular resolution of a radar system is determined by the beam steering step, which can be calculated from (3) for our system.

The bandwidth limit, on the other hand, is mostly limited by the opto-electronic devices used in the system, such as the MZM and the PD. In addition, the dispersion-induced power penalty [4] should also be considered as it may get significant due to the large equivalent dispersion of the recirculating dispersive loop [18]. To avoid the dispersion-induced power penalty, the spectrum of the microwave signal should be within the 3-dB bandwidth of the recirculating dispersive loop. Thus, it is required that the highest spectral component in the radar feed signal should satisfy [4]

$$f_{\max} < \sqrt{\frac{1}{8\pi N\beta}}. \tag{4}$$

It should be noted that the dispersion-induced power penalty can be completely eliminated by employing single-sideband with carrier (SSB+C) modulation [4], which is an effective way to overcome the bandwidth limitation imposed by (4).

III. Experiment

Two experiments are performed using two recirculating dispersive loops with each incorporating a different LCFBG with a different dispersion coefficient. The experimental setup is shown in Fig. 1 with a photograph shown in Fig. 3. First, the experiment is carried out using a recirculating dispersive loop with a large progressive time delay per round trip, i.e.,

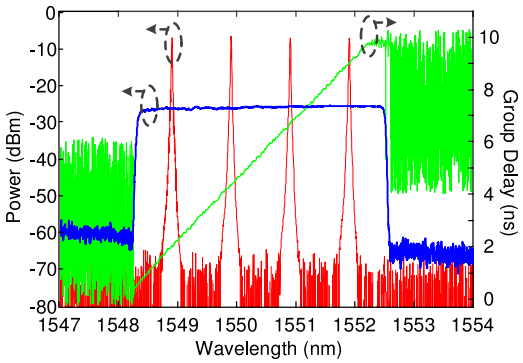

Fig. 4. The spectrum of the optical carriers at the output of WDM1 (red), the reflection power spectrum (blue) and the group delay response (green) of the LCFBG. The peak reflectivity of the LCFBG is 98%.

$\beta\Delta\lambda$ is chosen to be large. The central wavelengths of the four LDs (Agilent N7714A) are set to be 1548.9, 1549.9, 1550.9 and 1551.9 nm, with a uniform wavelength spacing of 1 nm. The OF is then programmed to have four 10-GHz-wide passbands at the same wavelengths. The optical spectrum of the wavelength-multiplexed optical carriers from the four LDs at the output of the WDM is shown in Fig. 4. Since the output power of a LD is independently tunable, a flat optical comb is generated. The LCFBG is fabricated to have a dispersion coefficient of 2500 ps/nm within its 4-nm reflection band centered at 1550.5 nm, which is also shown in Fig. 4. It can be calculated that $\beta\Delta\lambda = 2.5$ ns, i.e., a true-time delay difference of 2.5 ns can be achieved between two adjacent channels when the signal recirculates in the loop for one round trip. The AWG (Tektronix 7102), which has a sampling rate of 10 GSa/s, is configured to generate a microwave feed signal. A 2×2 coupler is used instead of the 2×2 switch to simplify the experiments and to study the round-trip-by-round-trip behavior of the system. Although the coupler cannot actively control the number of round trips for the optical signal to recirculate in the loop, part of the optical signal will be coupled out of the loop after each round trip, generating time-delayed signals with a uniformly increasing time delay difference between two microwave signals carried by two adjacent wavelengths. The time delays with a uniformly increasing time delay difference would induce a steering beam that scans over a certain range determined by the maximum value of N when the microwave is sent to a PAA. Note that the extra 3-dB loss introduced by the 2×2 coupler can be compensated by EDFA1 in the loop. The time-delayed signals are detected by four identical PDs with each having a bandwidth of over 20 GHz and sampled by a 4-channel oscilloscope (Agilent 93204A).

To demonstrate the generation of progressive time delays of the system, an electrical pulse with a temporal width of 1 ns is generated by the AWG, and applied to the MZM via the RF port. Four modulated optical signals are generated and sent to the dispersive loop to generate the required time delays. The waveforms detected at the outputs of the four PDs following the second WDM (WDM2) are shown in Fig. 5(a). Multiple time-delayed replicas of the electrical pulse are detected at the output of each channel with a repetition time of around 380 ns.

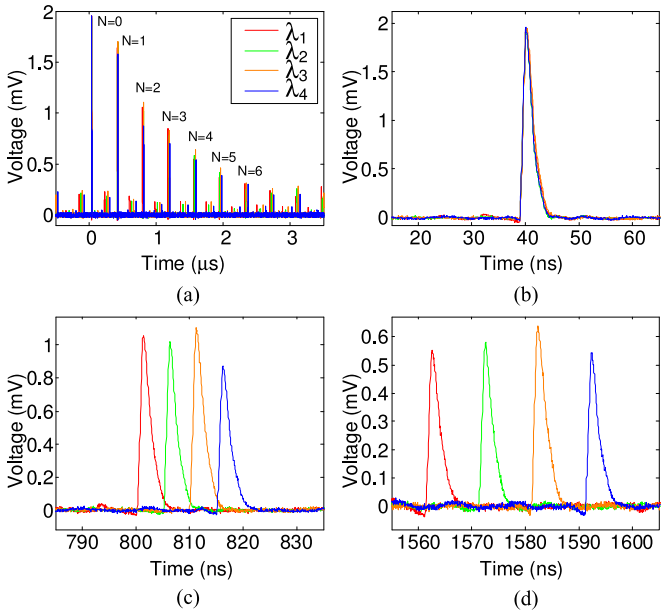

Fig. 5. Measured electrical signals at the outputs of the four PDs when an electrical pulse is applied to the MZM. (a) The generated time delayed replicas and the zoom-in view of the signals for (b) $N = 0$, (c) $N = 2$ and (d) $N = 4$.

In addition, the pulses from the four channels overlap in time only for $N = 0$ and an increasing time delay difference between two adjacent time-delayed pulses can be observed for $N > 0$, indicating that progressive true-time delays have been achieved for the channels when the optical pulses start to recirculate in the dispersive loop. Note that a reduction in the amplitudes of the time-delayed pulses as N increases is observed. This is because the gain of EDFA1 cannot be controlled to fully compensate for the loop loss, to avoid possible lasing at certain wavelengths. Nevertheless, the pulses can still recirculate for more than ten round trips before being imbedded in noise. The reduced amplitudes may be compensated by a microwave power amplifier that is commonly used in a PAA.

The higher frequency limit of the system for $N = 10$ is calculated to be 3.2 GHz by (4), which can be improved by using an LCFBG with a smaller dispersion coefficient, as will be shown later. Detected waveforms with more details are shown in Fig. 5(b)–(c) for different numbers of round trips of 0, 2 and 4. The time spacing between two pulses from two adjacent channels are measured to be 5.0 and 10.0 ns for $N = 2$ and $N = 4$, which are in perfect agreement with the theoretical value of 2.5 ns per round trip. Due to the relatively large progressive true-time delays, the system can be used for a PAA with a large element spacing and with a low operation frequency. Fig. 6 shows the calculated array factor of a four-element linear PAA, which has a uniform element spacing of 5 m and is driven by the time-delayed signals with different number of round trips. For $N = 0$, the beam is pointing to the broadside direction. An increment in the steering angle of 8.6° can be observed when the feed signal recirculates in the dispersive loop for one additional round trip, which is in good agreement with the theoretically calculated steering angle by (3). For four round trips, the beam

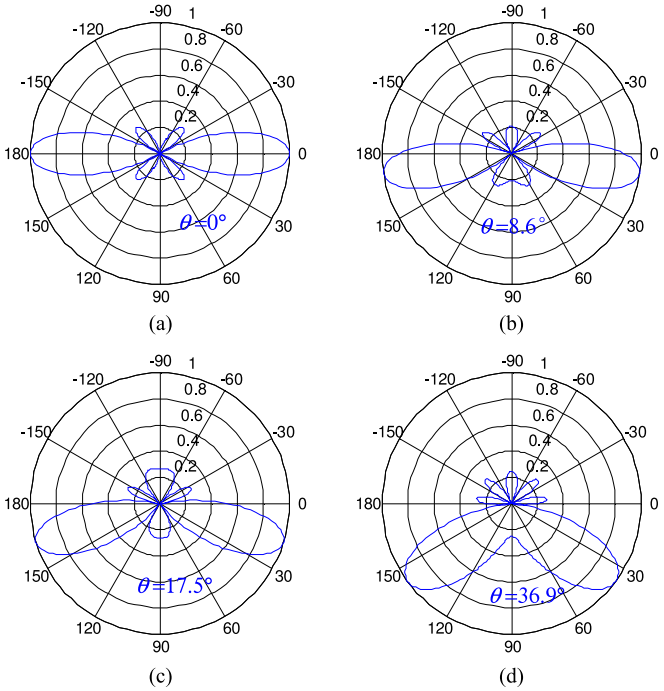

Fig. 6. Calculated array factors of a four-element linear PAA with an element spacing of 5 m. The array factor when the optical signals recirculate in the dispersive loop for (a) 0 round trip corresponding to a beam pointing direction of 0°, (b) 1 round trip corresponding to a beam pointing direction of 8.6°, (c) 2 round trips corresponding to a beam pointing direction of 17.5° and (d) 4 round trips corresponding to a beam pointing direction of 36.9°.

is pointing to 36.8°. It can be calculated that, if the number N can be controlled to be 12, the beam can be steered to cover a scanning range from –60° to 60°.

A linearly chirped microwave waveform (LCMW) with a large bandwidth and a long time duration is commonly used as a microwave feed signal [20]. To evaluate the performance of the system for a microwave signal with a large bandwidth and a long time duration, the AWG is configured to generate an LCMW with a large time duration of 300 ns and a chirp rate of 2 MHz/ns, with an instantaneous frequency starting from DC to 600 MHz. Fig. 7(a) shows the time-delayed signals at the outputs of the PDs. As can be seen again, a signal carried by a wavelength has a repetition time of 380 ns. The zoomed-in view of the signals after the optical signals recirculate in the dispersive loop for 0, 2 and 4 round trips are shown in Fig. 7(b)–(d). Again, progressive true-time delays can be observed, which again agree with the theoretical values. Since the time duration of the LCMW is shorter than the repetition time, the time delayed LCMWs do not overlap in time. Note also that a good signal-to-noise ratio is maintained even when the optical signals recirculate for more than 6 round trips in the dispersive loop.

For a given beam steering angle, different amount of progressive time delays are required for a PAA with different antenna element spacing. In our system, the true-time delays per round trip can be changed by using an LCFBG with a different dispersion coefficient or a laser array with a different wavelength spacing, according to (2). Here, an LCFBG with

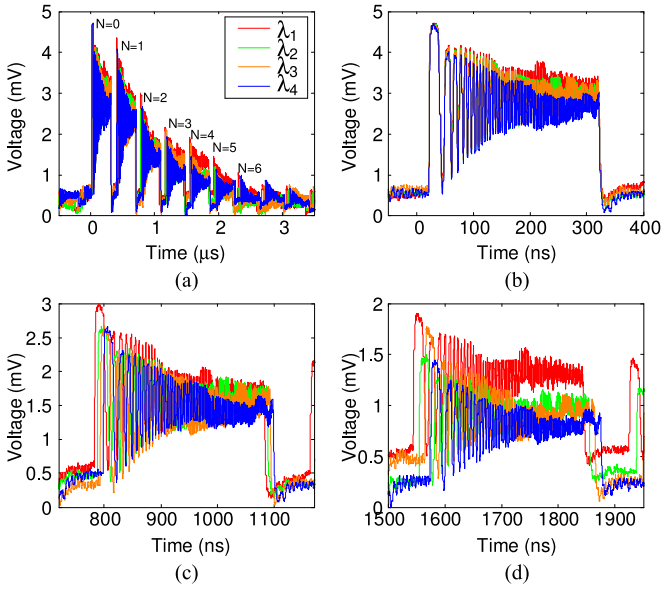

Fig. 7. Measured electrical signals at the outputs of the four PDs when an LCMW is applied to the MZM. (a) The generated time delayed replicas and the zoom-in view of the signals for (b) $N = 0$, (c) $N = 2$ and (d) $N = 4$.

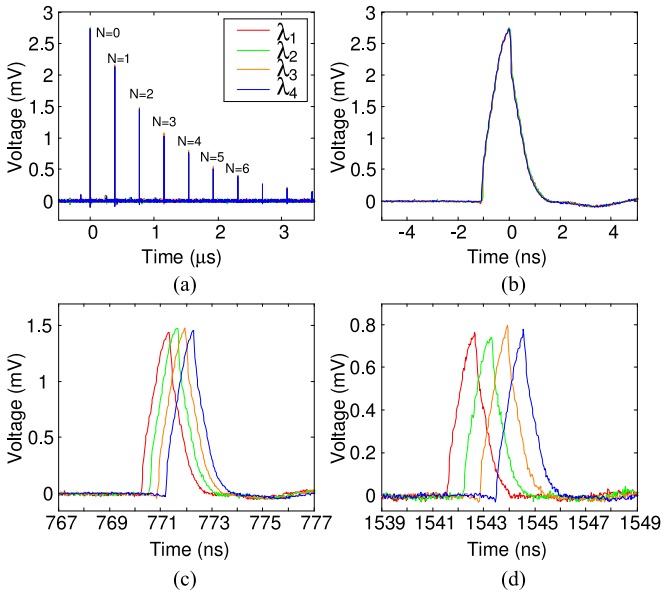

Fig. 8. Measured electrical signals at the outputs of the four PDs with a small true-time delay step of 160 ps. (a) The generated time delayed replicas and the zoom-in view of the signals for (b) $N = 0$, (c) $N = 2$ and (d) $N = 4$.

a smaller dispersion coefficient of 200 ps/nm is employed, and the wavelength spacing of the laser array is set at a fixed value of 0.8 nm. A true-time delay difference between two adjacent channels of 160 ps per round trip should be expected. Fig. 8 shows the measured time-delayed signals when a 1-ns electrical pulse is modulated on the multi-wavelength carriers. The measured true-time delay difference is 159.2 ps per round trip. Fig. 9 shows the calculated array factor of a four-element linear PAA with a uniform element spacing of 0.2 m when the time delayed signals are used to feed the antenna elements. Note that in the

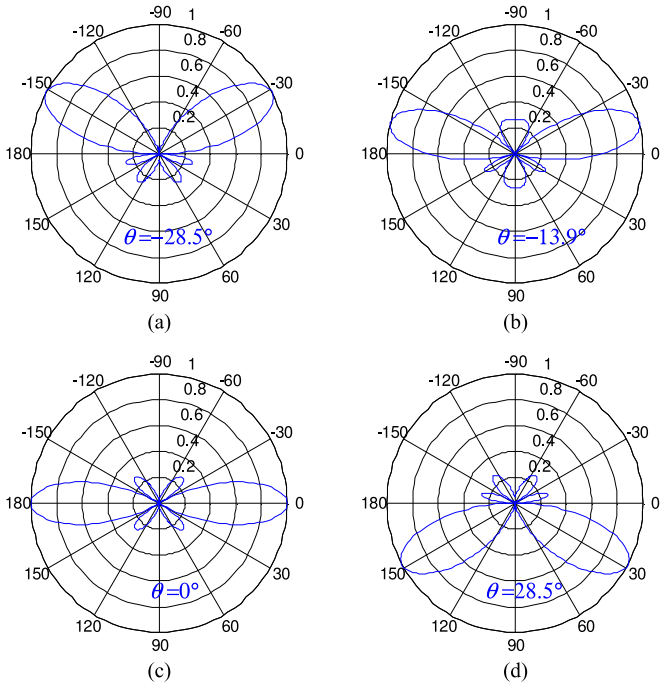

Fig. 9. Calculated array factors of a four-element linear PAA with an element spacing of 20 cm. The array factor when the optical signals recirculate in the dispersive loop for (a) 0 round trip corresponding to a beam pointing direction of –28.5°, (b) 1 round trip corresponding to a beam pointing direction of –13.9°, (c) 2 round trips corresponding to a beam pointing direction of 0° and (d) 4 round trips corresponding to a beam pointing direction of 28.5°.

calculation, an initial time delay difference is added so that the beam is pointing at –28.5° for $N = 0$. As the microwave feed signal recirculate in the loop for 1, 2 and 4 round trips, the beam is steered to –13.9°, 0° and 28.5°. The PAA can cover a steering range from –60° to 60° if the dispersive loop allows the optical signals to recirculate for over eight round trips. Assume that the signals recirculate in the loop for ten round trips, the higher frequency limit of the system is calculated to be 11.2 GHz according to (4), which is significantly higher than that when an LCFBG with a dispersion coefficient of 2500 ps/nm is used. It can be seen that, in order to implement broadband true-time delay system with large progressive time delays, a good solution is to use an LCFBG with a small dispersion coefficient and a laser array with a large wavelength spacing.

IV. Remarks

Note that the proposed beamforming system can be used to achieve tunable time delays for a pulsed signal. The pulse duration cannot be longer than the round trip time of the dispersive loop to avoid an overlap between two consecutive pulses. For a microwave signal with a longer temporal duration, the loop length should be longer. A longer dispersive loop will lead to a slower beam steering speed since the steering speed is limited by the over round trip time. For our proposed system, the total time for ten round trips is 3.8 μs, which is fast enough for most radar applications [21].

Note also that the system can generate true time delays for a PAA with non-uniform element spacing, which can be simply done by using a laser array with non-uniform wavelength spacing.

It should also be noted that the concept demonstrated here using a recirculating dispersive loop can be applied for many other applications where a large tunable time delay is needed.

V. Conclusion

In conclusion, we have proposed and experimentally demonstrated a photonic true-time delay beamforming network based on a switch-controlled wavelength-dependent recirculating dispersive loop. The microwave signal, with a temporal duration less than the round trip time of the dispersive loop, to be radiated to free space was modulated on the optical carriers of a laser array with fixed wavelengths. When the microwave-modulated optical signals recirculate in the dispersive loop, due to the wavelength-dependent time delays in the LCFBG, tunable progressive time delays could be achieved, which would lead to the beam steering when the time-delayed microwave signals are fed to a PAA. It is different from some previously reported techniques where the time delay tuning was realized by tuning the wavelength spacing of a laser array or the dispersion coefficient of an LCFBG, the system here is simpler since a laser array with fixed wavelengths is needed and the progressive time delays are generated and tuned by controlling the number of the round trips of the optical signals recirculating in the dispersive loop. The proposed true-time delay system was experimentally evaluated. In the experiment, an optical coupler instead of an optical switch was used to study the tunable time delay behavior of the system. Two true-time delay beamforming networks using two dispersive loops incorporating two different LCFBGs with dispersion coefficients of 2500 ps/nm and 200 ps/nm to achieve a time delay difference of 2.5 ns and 160 ps per round trip were demonstrated. The key advantage of the proposed approach is its simplicity for implementation since no TLA or tunable LCFBG is needed.

References

[1] A. W. Rihaczek, *Principles of High-Resolution Radar*. New York, NY, USA: McGraw-Hill, 1969.
[2] H. Shahoei and J. P. Yao, "Delay lines," *Wiley Encyclopedia Electr. Electron. Eng.*, pp. 1–15, Dec. 2014, doi: 10.1002/047134608X.W8234.
[3] J. Schwartz, Q. Zhuge, J. Azaña, and D. Plant, "1-D uniform and chirped electromagnetic bandgap structures in substrate integrated waveguides at 60 GHz," *Microw. Opt. Technol. Lett.*, vol. 54, no. 3, pp. 735–737, Mar. 2012.
[4] J. Yao, "Microwave photonics," *J. Lightw. Technol.*, vol. 27, no. 3, pp. 314–335, Feb. 2009.
[5] D. Dolfi, P. Joffre, J. Antoine, J.-P. Huignard, D. Philippet, and P. Granger, "Experimental demonstration of a phased-array antenna optically controlled with phase and time delays," *Appl. Opt.*, vol. 35, no. 26, pp. 5293–5300, Sep. 1996.
[6] Y. Liu, J. Yao, and J. Yang, "Wideband true-time-delay unit for phased array beamforming using discrete-chirped fiber grating prism," *Opt. Commun.*, vol. 207, no. 1, pp. 177–187, Jun. 2002.
[7] Y. Liu, J. Yang, and J. Yao, "Continuous true-time-delay beamforming for phased array antenna using a tunable chirped fiber grating delay line," *IEEE Photon. Technol. Lett.*, vol. 14, no. 8, pp. 1172–1174, Aug. 2002.

[8] D.-H. Yang and W.-P. Lin, "Phased-array beam steering using optical true time delay technique," *Opt. Commun.*, vol. 350, pp. 90–96, Sep. 2015.
[9] X. Ye, F. Zhang, and S. Pan, "Optical true time delay unit for multi-beamforming," *Opt. Express*, vol. 23, no. 8, pp. 10002–10008, Apr. 2015.
[10] Y. Minamoto and M. Matsuura, "True-time delay beamforming using semiconductor optical amplifier and tunable dispersion medium," in *Proc. IEEE Int. Conf. Netw. Infrastructure Digital Content*, 2014, pp. 164–167.
[11] S. Garcia and I. Gasulla, "Design of heterogeneous multicore fibers as sampled true-time delay lines," *Opt. Lett.*, vol. 40, no. 4, pp. 621–624, Feb. 2015.
[12] S. Chin *et al.*, "Broadband true time delay for microwave signal processing, using slow light based on stimulated Brillouin scattering in optical fibers," *Opt. Express*, vol. 18, no. 21. pp. 22599–22613, Oct. 2010.
[13] J. Wang *et al.*, "Continuous angle steering of an optically-controlled phased array antenna based on differential true time delay constituted by micro-optical components," *Opt. Express*, vol. 23, no. 7, pp. 9432–9439, Mar. 2015.
[14] L. Zhuang *et al.*, "On-chip microwave photonic beamformer circuits operating with phase modulation and direct detection," *Opt. Express*, vol. 22, no. 14, pp. 17079–17091, Jul. 2014.
[15] M. Burla *et al.*, "Multiwavelength-integrated optical beamformer based on wavelength division multiplexing for 2-D phased array antennas," *J. Lightw. Technol.*, vol. 32, no. 20, pp. 3509–3520, Oct. 2014.
[16] R. Bonjour, S. A. Gebrewold, D. Hillerkuss, C. Hafner, and J. Leuthold, "Continuously tunable true-time delays with ultra-low settling time," *Opt. Express*, vol. 23, no. 5, pp. 6952–6964, Feb. 2015.
[17] H. Lee, T. Chen, J. Li, O. Painter, and K. J. Vahala, "Ultra-low-loss optical delay line on a silicon chip," *Nature Commun.*, vol. 3, no. 5, pp. 1–7, May 2012, Art. no. 867.
[18] J. Zhang and J. Yao, "Time-stretched sampling of a fast microwave waveform based on the repetitive use of a linearly chirped fiber Bragg grating in a dispersive loop," *Optica*, vol. 1, no. 2, pp. 64–69, Aug. 2014.
[19] Q. Wang and J. Yao, "A high speed 2×2 electro-optic switch using a polarization modulator," *Opt. Express*, vol. 15, no. 25, pp. 16500–16505, Dec. 2007.
[20] J. Yao, "Photonic generation of microwave arbitrary waveforms," *Opt. Commun.*, vol. 284, no. 15, pp. 3723–3736, Jul. 2011
[21] A. Farina and P. Neri, "Multitarget interleaved tracking for phased-array radar," *IEE Proc.-F*, vol. 127, no. 4, pp. 312–318, Aug. 1980.

Jiejun Zhang (S'12) received the B.Eng. degree in electronic science and technology from the Harbin Institute of Technology, Harbin, China, in 2010, and the M.Sc. degree in optical engineering from the Huazhong University of Science and Technology, Wuhan, China. He is currently working toward the Ph.D. degree in electrical engineering at the Microwave Photonics Research Laboratory, School of Electrical Engineering and Computer Science, University of Ottawa, Ottawa, Canada.

His research interests include photonic generation of microwave waveforms, photonic processing of microwave signals, and fiber optic sensors.

Jianping Yao (M'99–SM'01–F'12) received the Ph.D. degree in electrical engineering from the Université de Toulon et du Var, France, in December 1997. He is a Professor and University Research Chair in the School of Electrical Engineering and Computer Science, University of Ottawa, Ottawa, Ontario, Canada. From 1998 to 2001, he was with the School of Electrical and Electronic Engineering, Nanyang Technological University, Singapore, as an Assistant Professor. In December 2001, he joined the School of Electrical Engineering and Computer Science, University of Ottawa, as an Assistant Professor, where he was promoted to an Associate Professor in 2003, and a Full Professor in 2006. He was appointed University Research Chair in Microwave Photonics in 2007. In June 2016, he was conferred the title of Distinguished University Professor of the University of Ottawa. From July 2007 to June 2010 and July 2013 to June 2016, he was the Director of the Ottawa-Carleton Institute for Electrical and Computer Engineering.

He has authored or coauthored more than 510 research papers, including more than 300 papers in peer-reviewed journals and 210 papers in conference proceedings. He is a Topical Editor for *Optics Letters*, and serves on the editorial boards of the IEEE TRANSACTIONS ON MICROWAVE THEORY AND TECHNIQUES, the *Optics Communications*, the *Frontiers of Optoelectronics*, and the *Science Bulletin*. He was as a Guest Coeditor for a Focus Issue on Microwave Photonics in the *Optics Express* in 2013 and a Lead-Editor for a Feature Issue on Microwave Photonics in *Photonics Research* in 2014. He is a Chair of numerous international conferences, symposia, and workshops, including the Vice Technical Program Committee (TPC) Chair of the IEEE Microwave Photonics Conference in 2007, TPC Co-Chair of the Asia-Pacific Microwave Photonics Conference in 2009 and 2010, TPC Chair of the high-speed and broadband wireless technologies subcommittee of the IEEE Radio Wireless Symposium in 2009-2012, TPC Chair of the microwave photonics subcommittee of the IEEE Photonics Society Annual Meeting in 2009, TPC Chair of the IEEE Microwave Photonics Conference in 2010, General Cochair of the IEEE Microwave Photonics Conference in 2011, TPC Cochair of the IEEE Microwave Photonics Conference in 2014, and General Cochair of the IEEE Microwave Photonics Conference in 2015. He is also a Committee Member of numerous international conferences, such as IPC, OFC, BGPP, and MWP. He received the 2005 International Creative Research Award of the University of Ottawa. He recived the 2007 George S. Glinski Award for Excellence in Research. In 2008, he was awarded a Natural Sciences and Engineering Research Council of Canada Discovery Accelerator Supplements Award. He was selected to receive an inaugural Optical Society of America (OSA) Outstanding Reviewer Award in 2012. He was an IEEE MTT-S Distinguished Microwave Lecturer for 2013-2015.

He is a registered Professional Engineer of Ontario. He is a Fellow of the OSA, and the Canadian Academy of Engineering.